inter.noise
HAMBURG 2016

Measurement of the spatial sound propagation with a low-cost sound intensity scanner

T. B. Klaus[1], M. Schmidt and S. Herold
Fraunhofer Institute for Structural Durability and System Reliability LBF
Darmstadt, Germany

ABSTRACT
Sound waves are compression oscillations propagating in an acoustic fluid. The fluid possesses kinetic energy by means of volume flows and potential energy in terms of pressure. These entities are characterized due to the physical dimension of the sound intensity. Hereby, the acoustic radiation of noise sources such as vibrating structures can be described. As the sound intensity is a vectorial dimension it is possible to describe the magnitude of the radiation in terms of the sound-pressure or power and the direction of propagation by the power fluxes. Acquiring the three dimensional sound intensity in a spatial domain is a time- and cost-intensive procedure, based on the state-of-the-art measurement equipment. By this means a low-cost setup is introduced, consisting of the three dimensional sound-intensity-probe and the positioning unit. Hereby, the automated characterization of noise sources and the identification of acoustic hot spots are possible. The probe is implemented by means of electret capsules. Furthermore, the step-motor driven positioning unit is controlled by an Arduino DSP board. The system is compared to standard methods for the estimation of the sound-power and an alternative pu-sound intensity probe, with respect to correction factors improving system inherent errors of pp-probes.

Keywords: sound, noise propagation measurement, sound intensity, low-cost, spatial energy flow

1. INTRODUCTION

Sound waves are defined as compression oscillations that propagate in an acoustic fluid [1]. The moving fluid possesses hereby kinetic energy in form of flows and potential energy in terms of pressure. This measures can are depicted by the acoustic sound-intensity for a radiating structure. The sound-intensity is a vectorial quantity and describes the radiated sound-power as well as the direction of propagation in the three dimensional spatial domain. Conventional systems for the determination consist of a probe, which has to be operated by hand. By this means the measurement of large machines is quite time consuming. The manual operation also means a negative impact on the quality of the measurement results. In addition the probes are quite expensive and so it is hard to work in a polluted environment (e.g. by oil or dust), because the probe may be damaged. By this means this work focusses on the design and implementation of a low-cost system for the automated measurement of the spatial distributed sound intensity.

First considerations of the sound intensity were made by RAYLEIGH [2]. Because of the low computational power in year 1970 a direct measurement of the sound-intensity was not possible. Since modern digital signal processing and reliable microphones are available the direct measurement is possible. This progress was highly influenced by the work of FAHY [1]. Nowadays, diverse commercial systems are available for the measurement of the sound intensity in the one and three- dimensional domain. For an evaluation with state-of-the-art probes and an estimation of the systematic errors the considered intensity-probe is compared to a pu-probe of the company Microflown. In addition the measured sound-power of a settlement noise source will be evaluated.

[1]email: tim.bastian.klaus@lbf.fraunhofer.de

2. THEORY

2.1 Definition of the sound intensity and the sound-power

The vectorial sound intensity is described as the average amount of the sound-power propagating through a unit area [3]. This can be defined with the product of the instantaneous sound-power $p(t)$ and the particle-velocity $u(t)$

$$I_s = \frac{1}{T_{int}} \int_0^{T_{int}} p(t)u(t)\mathrm{d}t, \tag{1}$$

over the integration time range T_{int}. For the steady-state equation (1) can be expressed in the complex representation

$$I_s = \frac{1}{2}\Re\left\{p^*(r) \cdot u(r)\right\} = \frac{1}{2}\Re\left\{p(r) \cdot u^*(r)\right\}, \tag{2}$$

where $p(r)$ and $u(r)$ match the sound pressure and particle velocity at the position r, with the complex conjugate indicated with * [4].

The sound intensity can be split in the *active* and *reactive* parts. The active part represents the important one, which is determined through experimental measurements of the sound-intensity. The reactive part is neglected. Nevertheless, also the reactive part is of interest, as the radiated sound field can be described by both proportions. A classification can be made by an evaluation of the particle velocity and the sound pressure [5]. For the active part the particle velocity is in-phase with the sound pressure. The reactive part has a phase difference of 90°. By this means the average value of the reactive intensity is zero. This consideration can be utilized for the classification in near and far field of the radiated source. In the near field the reactive part dominates, based on the phase difference of sound pressure and particle velocity. With a gaining distance the reactive part decays until the active part dominates.

The radiated sound-power can be measured with various methods. In this work the *sound intensity method* is carried out and compared to the results of the *sound-pressure*, which is measured in an anechoic chamber. Both methods are based on the same theoretical basics [6]. If the sound intensity of a radiating structure is

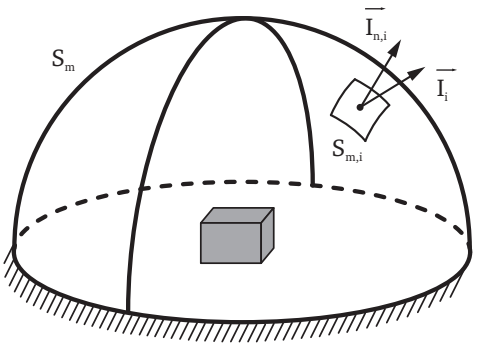

Figure 1. Enveloping surface for sound-power measurement based on the sound-intensity

measured on a closed half sphere (see Figure 1). The integral of the perpendicular component of the three dimensional vector of the intensity $\overrightarrow{I_n}$ over the enveloping surface S results to the sound-power

$$P = \int_{S_m} \overrightarrow{I_n}\mathrm{d}S. \tag{3}$$

In this article the discrete measurement procedure is used. But also scanning or continuous methods are possible [7]. As enveloping surface a cuboid is used, whereby also a sphere or cylinder would be possible. For each segment the partial power is measured based on the product of the normal intensity with the surface and summed up

$$P = \sum_i^N I_{n,i} \cdot S_{m,i} \tag{4}$$

to the overall sound-power. The main advantage of this approach is that only sources inside the enveloped surface are measured. Entering proportions exit the volume on the diametric opposite side, whereby entering and exiting parts cancel out. Therefore, this method is also applicable in rooms with no free field conditions and adjacent noise sources, which are then neglected during the measurements.

The alternative method for the estimation of the radiated sound-power is the measurement of the sound pressure on a sphere around the source. For this purpose, the source is seen as an point-source, where the sound pressure is measured in the far field. Sound pressure and particle velocity are in phase and the intensity can be rewritten as

$$I_s = \frac{1}{2}\frac{p^2}{\rho c_0}. \tag{5}$$

The evaluation of the sound-power in non-echoic chambers with measurements of the sound-pressure is defined by DIN EN ISO 3744 und DIN EN ISO 3745 [8, 9]. In this work a spherical measurement surface is used, which is appropriate for a broadband sound-source. Here, the source has to be placed in the center. The radius value must be chosen in the range of 1-16 m and shows a minimum distance of twice the characteristic source dimensions. Based on the dimensions of the used sound source also a radius value below 1 m is appropriate if it has minimum distance of 0.5 m in order to achieve an unbounded frequency domain.

2.2 Measurement of the three-dimensional sound-intensity

For the experimental evaluation of the sound-intensity, both the sound power and particle velocity are needed. A basic differentiation for the direct measurement of the sound-intensity can be made by the classification in *pu-probes* and *pp-probes*. Pu-probes measure the particle-velocity directly with a hot-wire sensor and pp-probes use two pressure microphones to calculate the particle-velocity out of numerical differentiation. In general, pu-probes show a filigree setup that makes the sensors quite sensitive and expensive. Basically, pp-probes show a numerical approximation error based on the distance of the microphones. In this article a pp-probe is considered, because it can be used quite well for the design of a low-cost sound intensity probe.

The calculation of the sound intensity in the time and frequency domain is defined as the product of the sound pressure and the particle velocity [1]. Based on the three dimensional linearized conservation of momentum

$$\rho\frac{\partial \boldsymbol{v}}{\partial t} + \boldsymbol{p} = 0, \tag{6}$$

and the conservation of the masses

$$\frac{\partial \rho}{\partial t} + \rho\boldsymbol{v} = 0, \tag{7}$$

which represent Euler's equations, the particle velocity can be calculated with

$$\frac{\partial p}{\partial n} = -\rho\frac{\partial v_n}{\partial t} \tag{8}$$

in an arbitrary direction n. By this means the particle velocity can be evaluated with the time integral

$$v_n(t) \approx \frac{1}{\rho d_n}\int_{-\infty}^{t} \left[p_1(\tau) - p_2(\tau)\right] \mathrm{d}\tau, \tag{9}$$

with the distance d_n between the acoustic centers of both two microphones. The sound pressure is the arithmetic mean value of the microphones

$$p(t) \approx \frac{1}{2}\left[p_1(t) + p_2(t)\right]. \tag{10}$$

The product of equation (9) and (10) results to the instantaneous sound intensity

$$I_n(t) \approx \frac{1}{2}\frac{1}{\rho d_n}\left[p_1(t) + p_2(t)\right]\int_{-\infty}^{t}\left[p_1(\tau) - p_2(\tau)\right]\mathrm{d}\tau. \tag{11}$$

In case of steady-state sound fields the evaluation of the frequency domain is tendering. Thereby, the cross-power spectrum of the microphone signals results to the intensity with

$$I_n(\omega) = -\frac{1}{\rho\omega d_n}\Im\left\{G_{p1,p2}(\omega)\right\}. \tag{12}$$

3. IMPLEMENTATION OF THE SOUND INTENSITY SCANNER

3.1 Design of the sound intensity probe

Figure 2 shows an overview of possible orientation setups for pp-probes. In this article the *back-to-back* orientation is used to allow an uniform sound incidence to the microphones and avoidance of diffraction phenomena. Furthermore, the orientation of the microphones for the measurements of the three dimensional

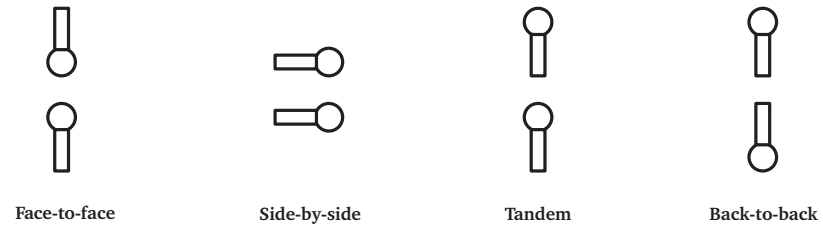

Figure 2. Schematic microphone orientation of pp-intensity probes

sound intensity is important. Different microphone setups have been investigated by the companies Ono Sokki, Brüel & Kjaer and GRAS [10]. As a result, the most common setups use four or six microphones. Like illustrated in figure 3, a cubic or tetrahedral setup with four microphones or a centralized one with six microphones is possible. For the four microphone variations the acoustic centers lay either in one of the room corners or the geometric center. For a more explicit definition of the spatial directions in space the six microphone variant is used, even as additional microphones are necessary. The designed low-cost probe is shown in figure 4. The configuration corresponds to figure 3 (right) with the implementation of two microphones in each spatial direction with a distance of 25 mm.

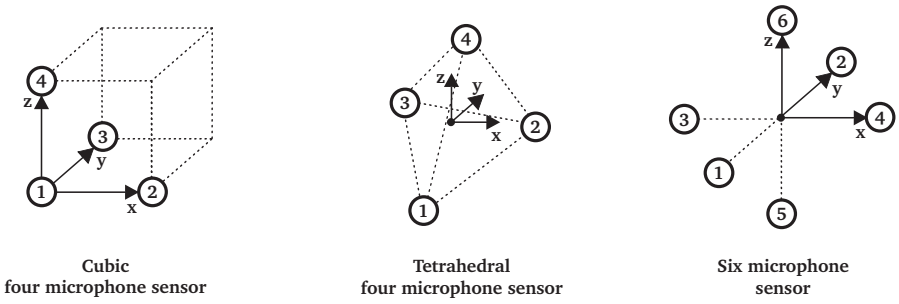

Figure 3. Schematic microphone orientation of 3D-pp-intensity probes

Figure 4. Three-dimensional low-cost pp-probe

3.2 Evaluation of a suitable acoustic transducer

The exact measurement of the sound pressure is fundamental for a correct estimation of the sound intensity with a pp-probe. Therefore, the most suitable low-cost microphone has to be chosen for this purpose. Three different acoustic transducers are compared in this section. The specifications of the transducers are listed in table 1. The laboratory microphone is used as a benchmark for the comparison of a commercial electret capsule and a MEMS-microphone. A detailed description of the transducers can be found in the literature [6, 11–13]. The laboratory microphones are of the type PCB T130D21. The low-cost electret capsules are type KECG2742PBL-A from Kingstate and the MEMS are type SPM0204HE5 of the brand Knowles Acoustics. A special focus is set to electret capsules, as they turn out as best solution for the intensity probe in terms of dimensions and measurement accuracy also with respect to the costs.

Parameter	**Laboratory-**	**Electret-**	**MEMS-microphone**
Direction	Free-field	Omni-directional	Omni-directional
Frequency domain (-2 to 5 dB)	20 - 15 kHz	20 - 20 kHz	100 - 8 kHz
Phase deviation	$\pm 5°$	-	-
Sensitivity ($\pm$3 dB re 1 $\frac{V}{Pa}$ @ 1 kHz)	-26.9 dB	-42.0 dB	-42.0 dB
Floor noise	<30 dB	-	35 dB
Signal-to-noise ratio	-	58 dB	59 dB
Supply voltage	18-30 VDC	2 VDC	1.5-3.6 VDC
Output resistance	70 Ω	2.2 kΩ	300 Ω
Dimension	7×81.8 mm^2	6×2.7 mm^2	$4.72 \times 3{,}76 \times 1{,}25$ mm^3
Weight	5.40 g	0.17 g	0.07 g

Table 1. Specification of the investigated microphones

For the choice of the most suitable low-cost sensor a qualitative evaluation of the electret and MEMS microphone has to be performed with respect to the high quality laboratory microphone. By this means an experimental setup is used, where a volume-source is placed in the spatial center of an anechoic room. The microphones are placed 500 mm above the source and the frequency response function is evaluated with a sweep excitation in the range of 100 Hz to 1000 Hz. It is possible to compare the measured signals in free-field conditions. For an evaluation of the sensor signals the frequency response deviation with regard to the

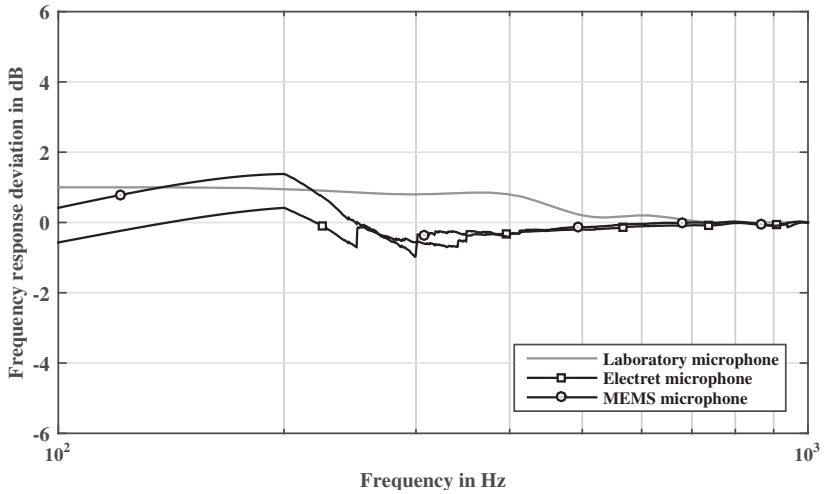

Figure 5. Sensitivity of the investigated microphones

sensitivity at 1000 Hz in figure 5 and the coherence of the measured signal compared to the volume- displacement sensor signal of the Q-source in figure 6 are evaluated. In relation to the frequency response the electret

microphone shows a sensitivity of $2,551 \cdot 10^{-4}$ V/Pa and the MEMS-microphone $2,815 \cdot 10^{-4}$ V/Pa for an amplitude of 0 dB at 1000 Hz. Similar to the laboratory microphone, the considered low-cost microphones show a constant measured sensitivity in the regarded frequency range (figure 5). The mean deviation of the electret-microphone shows the lowest value with 0.19 dB. But also the MEMS- microphone results in a lower value of 0.26 dB than the laboratory microphone with 0.38 dB. With a special focus on the frequency domain the low-cost microphones show a constant sensitivity above 300 Hz.

Furthermore, the evaluation of the coherence of the microphone signals with respect to the reference signal of the volume-displacement of the source is considered. In figure 6 it can be noticed, that the laboratory microphone shows an excellent coherence above 150 Hz. The drops can be accounted especially to the poor quality of the reference signal in this range. Investigating the results of the electret microphone the cut-off frequency increases to a frequency of 170 Hz. The effect is even clearer comparing the moving average, which lies below the mean average of the laboratory microphone. The limit is even increased when the signal of the MEMS microphone is regarded. Here, the moving average lies below the other two microphones.

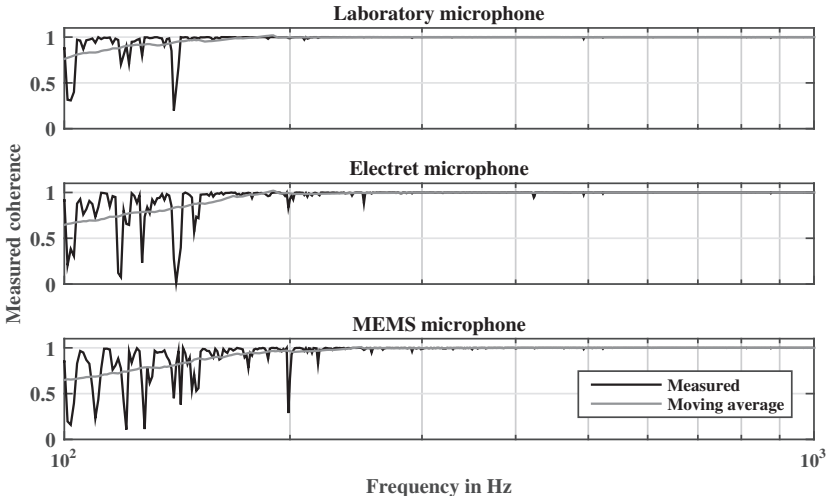

Figure 6. Coherence of the investigated microphones

Summing up the results of both investigations, one can say, that the laboratory microphone shows best results especially for the coherence of the measured signal. For the mean frequency response deviation all three microphones show similar results, whereby the electret microphone shows the best results. Therefore, the electret microphone emphasizes as a suitable alternative for the laboratory microphone considering an implementation in the low-cost sound intensity probe. Although the MEMS microphone shows only slight disadvantages.

3.3 Improvement of system inherent errors of the measured sound intensity

The scientific field of sound intensity probes was investigated over the last decades. During this period a lot of work addresses the quantification of error sources measuring the sound intensity [14–16]. At this point only the major important errors are addressed with a special focus on pp-probes. Regarding pu-probes the literature is referenced in [1]. A fundamental differentiation can be made in *instrumentation*, *measurement* and *numerical errors*. Instrumentation errors address the influence of the microphones to the sound field. This effect is important in the higher kHz frequency range. For the acoustical domain below 20 kHz the influence can be neglected. Measurement errors consider stochastic influences that can be reducible to the phase-difference of the micro- phones and the environmental conditions [17]. For a reduction of stochastic effects a high averaging time of 20 s is recommended, whereby the distance to the radiating structure should not fall below 200 mm preventing nearfield effects. The influence of adjacent error sources and the phase difference of the microphones can be quantified with

$$\hat{P}_a \simeq P_a - \frac{\varphi_e}{k\Delta r} \int_S \left(\overline{p^2}/\rho c_0 \right), \tag{13}$$

whereby the error of the measured sound-power is proportional to the phase-difference φ_e and the mean sound-power $\overline{p^2}$ of the surrounding environment. Therefore, the measurements are performed in an anechoic

chamber reducing the influence of surrounding sound fields. In idealized considerations phaseangles of the microphones are neglected. Reality shows that even high class laboratory microphones bear a phase difference of up to 5 °. For this reason the used low-cost microphones are tested and matched so they show a maximum phase difference of 5 ° in the regarded frequency domain up to 1000 Hz.

The most serious error is affected by the numerical calculation of the particle velocity in equation (9) based on the spatial derivation between the microphones. Here, the assumption is made, that the sound-pressure is linear between the microphones. This means that the quality of the approximation is increased for a decreasing distance of the microphones [18, 19]. In this context, the relation of the approximated sound intensity $\hat{I}$ and the real intensity I can be calculated to

$$\frac{\hat{I}}{I} = \frac{\sin(k\Delta r)}{k\Delta r} \tag{14}$$

with respect to the relation of frequency and microphone distance $k\Delta r$. For the regarded pp-probe an upper limit frequency of approximately 6.5 kHz can be calculated, if only two microphones in each spatial direction are considered. It follows that the error of the numerical differentiation tends to zero if the distance of the microphones also goes to zero. As for real probes a low distance is not easy to manufacture the calculations of the intensity have to be customized in terms of an improvement of the measurements. First equation (12) is extended to

$$I_x(\omega) = -\frac{1}{\rho\omega d_x}\frac{1}{5}\Im\left\{G_{p3,p4} + G_{p3,p1} + G_{p1,p4} + G_{p3,p2} + G_{p2,p4} + \ldots + G_{p3,p5} + G_{p5,p4} + G_{p3,p6} + G_{p6,p4}\right\} \tag{15}$$

$$I_y(\omega) = -\frac{1}{\rho\omega d_y}\frac{1}{5}\Im\left\{G_{p1,p2} + G_{p1,p3} + G_{p3,p2} + G_{p1,p4} + G_{p4,p2} + \ldots + G_{p1,p5} + G_{p5,p2} + G_{p1,p6} + G_{p6,p2}\right\} \tag{16}$$

$$I_z(\omega) = -\frac{1}{\rho\omega d_z}\frac{1}{5}\Im\left\{G_{p5,p6} + G_{p5,p1} + G_{p1,p6} + G_{p5,p2} + G_{p2,p6} + \ldots + G_{p5,p3} + G_{p3,p6} + G_{p5,p4} + G_{p4,p6}\right\} \tag{17}$$

with respect to the cross-power spectra shares of all microphone positions. With this extended calculation in all three spatial directions the numerical distance of the microphones can be decreased with a resulting higher limit frequency of approximately 9.7 kHz. The corresponding microphone positions can be seen in figure 4. Furthermore, the measured sound intensity can be corrected using equation (14) regarding to the numerical error drops. The resulting corrections are compared to commercial sound intensity and power measurement methods in the following section.

3.4 Design of the sound intensity scanner

Manual measurements of the radiated sound-power using handheld sound intensity probes are a time consuming procedure. Furthermore, the positioning repeatability is not guaranteed because of a lack of accuracy caused by manual operation. Therefore, the low-cost sound intensity probe operates within a portal system to ensure a high position accuracy regarding the measurement points. The design of the whole system is shown in figure 7. The drive unit is mounted on a solid aluminum base frame with the dimensions of 2000x2000x2700 mm^3. Due to the translational movement of the sound intensity probe by three step-motors, every position within the portal system can be approached. The control of the scanning unit is done by a digital signal processing (DSP) board *Arduino Due* that is operated with a graphical user interface in MATLAB. The measurement positions are defined in an Excel table which can be imported into MATLAB. For the communication between MATLAB and the DSP board a serial port is established. After the initiation process for the start position of the probe, every desired measurement position in x-, y- and z-direction can be approached through the drive of the step-motors. If the position is reached, a trigger signal indicates the start for the signal acquisition hardware. This process is repeated until the whole area of the intensity field is measured.

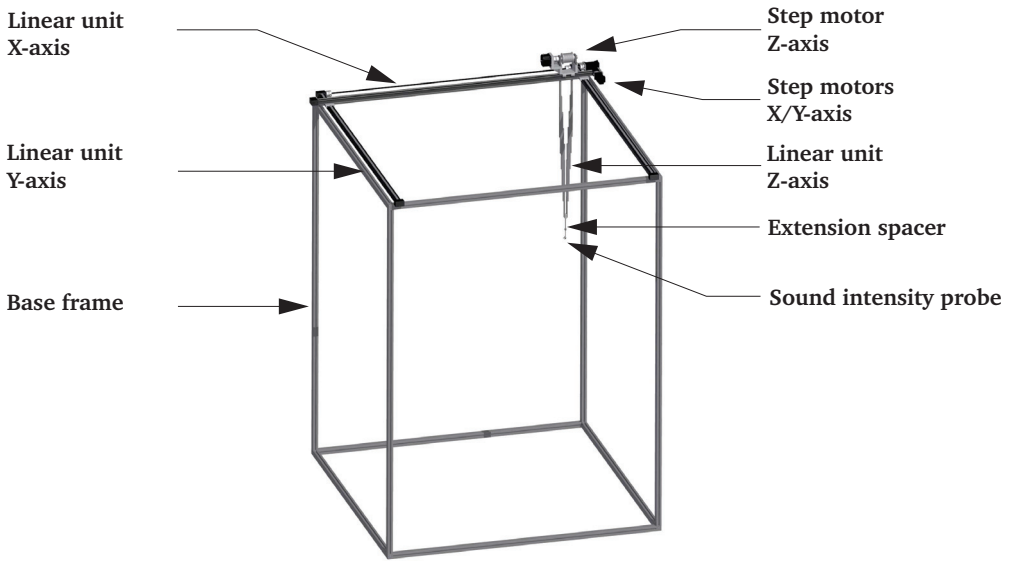

Figure 7. Portal system of the sound-intensity scanner

4. MEASUREMENTS

4.1 Evaluation based on available commercial sound intensity sensors

The evaluation process for the portal system consists of a result comparison of the sound intensity measurements with respect to DIN EN ISO 9614-1 compared to the sound-power measurements according to DIN EN ISO 3744 and DIN EN ISO 3745 [7–9]. The reference source type 4204 of the company Brüel & Kjaer is considered, which consists of a radial fan driven by an asynchronous motor. This source fulfills requirements according to ISO 3741, ISO 3747 and ISO 6926 as calibrated sound-power source. In this context, the calibration data is also at hand in terms of terce spectra.

As first step of the evaluation the radiated sound-power of the reference source is measured due to the sound pressure method. By this means a microphone array of 20 laboratory microphones is placed on a spherical surface with a diameter of 1.5 m around the source in an anechoic chamber. Also reference measurements are performed with a Microflown pu-probe. This is a commercial probe, where the one dimensional sound intensity is directly measured in terms of a microphone and the particle velocity with a heat-wire-anemometer [20]. This device measures the fluctuation of the air-mass based on two wires made of platinum, which detect temperature differences with respect to adjacent air flows. Three dimensional measurements are performed by a rotation in the required spatial coordinate direction. Even though also pu- probes underlie system inherent errors based on a phase-difference of both sensors. They result in errors regarding the reactive and active power. As state-of-the-art sensors they show the best results and serve here as reference for the measured sound intensity with the low-cost probe. The behavior of pu-probes is well known and documented in literature [21].

The sound intensity is measured with the low-cost probe on a cubic enveloping surface with the dimensions of 1200x1200x800 mm^3. Herby, the standardized minimum distance of 500 mm from the reference source is kept. In this context the sound-power is evaluated on measurement areas with the dimensions 200x200 mm^2. The perpendicular sound-intensity vector is measured at the center of the area. For an evaluation of the measurement data based on the sound-power method, the pu- and pp-probe are compared to the calibration data of the reference source in figure 8. It can be noticed, that all measurement methods fit the calibration data quite accurate until a frequency of 3 kHz. Furthermore, the sound-power shows a divergence in the frequency range of 3 kHz to 7 kHz and 11 kHz to 18 kHz. The reason for that is the vertical fluctuation of 6 dB, which is documented in the data-sheet of the reference source in this frequency range and the relatively low number of 20 microphones needed by the norm. Nevertheless, the summed sound-power results to 93.2 dB compared to the reference value of 92.4 dB. At this point the pu-probe shows a lower divergence

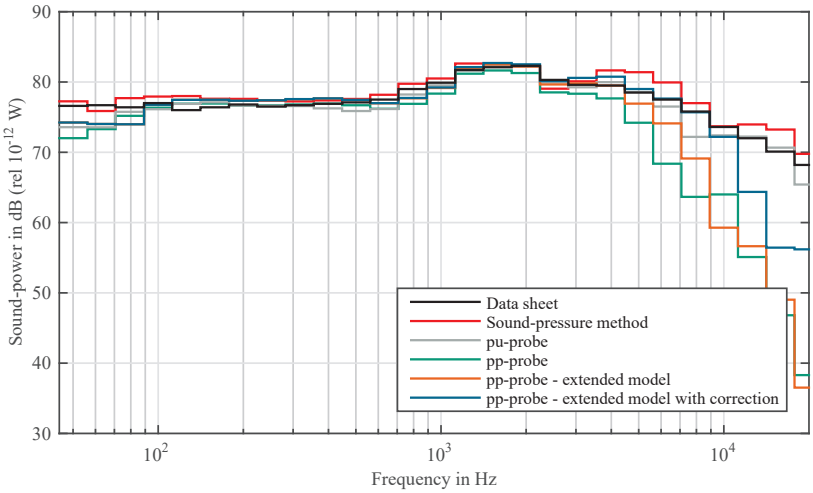

Figure 8. Evaluation of the measured sound-power of the reference source in terces

of 0.4 dB regarding to the reference value with 92.0 dB. Only below 100 Hz a drop of the measured sound-power can be noticed, which can be traced back to the system inherent low sensitivity with a trend of 6 dB per octave [21]. Furthermore, the narrow band evaluation in figure 9 shows a drop at 14 kHz based on the

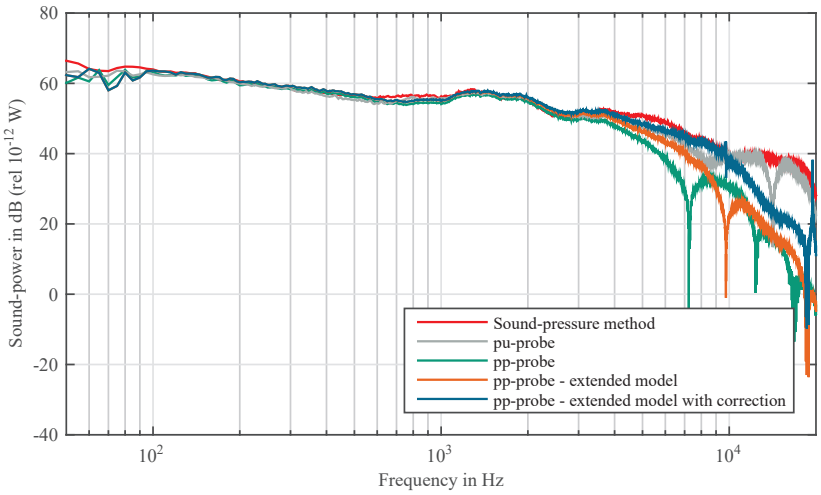

Figure 9. Narrow band evaluation of the measured sound-power of the reference source

phase divergence of the sound pressure und particle velocity sensor. But this has only a small impact on the results in terces (see figure 8).

By comparison of the results of the pp-probe it can be noticed, that with a summed sound-power level of 91.0 dB adequate results are established with the low-cost sensor. Similar to the pu-probe the pp-probe shows a slight drop below 100 Hz. This can be addressed to the low coherence of the electret microphones in this frequency range (see figure 6). More serious influences to the measurements occur by the numerical approximation of the particle velocity resulting in a divergence over 4 kHz for the measured sound-power. Therefore, the previously proposed correction is recommended. Considering the extended calculation method in equations (15) to (17) the possible and verified frequency range can be increased up to 9.7 kHz (see figures 8 and 9). The resulting summed sound-power level is 92 dB. Furthermore, the application of the correction in equation (14) results in an additional improvement increasing the valid frequency range to a limit frequency of approximately 10 kHz. Due to this fact, the summed sound-power can be calculated to 92.5 dB resulting in the lowest deviation of the referenced value of all the proposed methods.

4.2 Measurement of energy flow

The automation of the sound intensity measurement allows the scanning of a three dimensional volume with a high density of measurement points. Considering a steady-state sound field the sound propagation can be visualized due to the sound energy flow based on the averaged intensity. In figure 10, the continuous propagation for the reference source is pictured. The lines follow the tangential of the vector field by which the wave front propagates orthogonally. Besides the representation of noise sources and sinks are possible. The visualization of the propagation paths regarding to the color scale defines the absolute amplitude of the

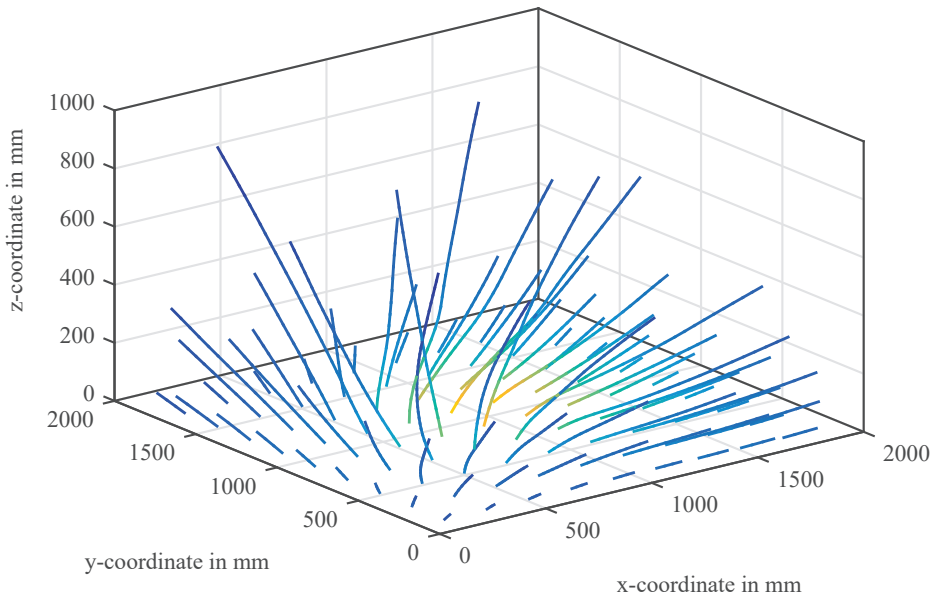

Figure 10. Energy flow of the reference source

sound intensity. It can be seen, that the highest energy occurs in the area of the reference source. Furthermore, the level of the paths implies that radiated sound in the nearfield propagates starting from the moving direction of the radial moving blades of the source. With an increasing distance to the source the propagation paths show an uniform trend outwards with spherical characteristic of a point source in the far field. With this visualization it is now possible to identify hot-spots of a radiating structure in order to optimize the sound radiation of structures.

5. CONCLUSION

The design and implementation of a three dimensional pp-probe has been shown in terms of a sound intensity scanning device. The low-cost setup was compared to state-of-the art techniques for the determination of the sound intensity in form of a commercial pu-probe and a standardized sound-power measurement setup. The evaluation is based on an acoustic reference source. It was possible to validate the function of the low-cost system. Nevertheless, the probe shows system inherent errors, which can be improved by the introduction of an extended method of the sound intensity implying all six microphones in the calculation of the sound intensity in each spatial direction. Furthermore, the results are improved by a correction factor based on the numerical error estimation based on the distance of the microphones. The gained measurement results reflect the calibration and measured data adequate. Also a further improvement accounting the reproducibility and the conduction of the measurements could be achieved by the automation of the measurement. Therefore, also the measurement of the acoustic energy flow is possible with a minimization of effort and time. In general, the identification of acoustic hot-spots and the determination of the acoustic propagation paths in the three-dimensional spatial domain is possible. Finally, with the choice of low-cost elements a sound intensity measurement device can be established, which is suitable for the adequate measurement of the radiated sound field even for complicated environmental conditions.

REFERENCES

[1] Frank Fahy. *Sound intensity*. CRC Press, 2002.

[2] John William Strutt Baron Rayleigh. *The theory of sound - Volume 1*, volume 1. Macmillian and Co. London, 1877.

[3] Deutsches Institut für Normung e.V. DIN EN ISO 15186-1 - Akustik - Bestimmung der Schalldämmung in Gebäuden und von Bauteilen aus Schallintensitätsmessungen - Teil 1: Messungen im Prüfstand. Beuth, Dezember 2003.

[4] P. A. Nelson and S.J. Elliot. *Active Control of Sound*. Academic Press, 1992.

[5] S. Gade. Sound intensity (part i theory). *Briiel & Kjaer Technical Review 3*, 1982.

[6] Franz G. Kollmann, Thomas F. Schösser, and Roland Angert. *Praktische Maschinenakustik*. Springer / VDI, 2006.

[7] Deutsches Institut für Normung e.V. DIN EN ISO 9614-1 - Akustik - Bestimmung der Schallleistungspegel von Geräuschquellen aus Schallintensitätsmessungen - Teil 1: Messungen an diskreten Punkten. Beuth, November 2009.

[8] Deutsches Institut für Normung e.V. DIN EN ISO 3744 - Akustik - Bestimmung der Schallleistungs- und Schallenergiepegel von Geräuschquellen aus Schalldruckmessungen - Hüllflächenverfahren der Genauigkeitsklasse 2 für ein im Wesentlichen freies Schallfeld über einer reflektierenden Ebene. Beuth, Februar 2011.

[9] Deutsches Institut für Normung e.V. DIN EN ISO 3745 - Akustik - Bestimmung der Schallleistungs- und Schallenergiepegel von Geräuschquellen aus Schalldruckmessungen - Verfahren der Genauigkeitsklasse 1 für reflexionsarme Räume und Halbräume. Beuth, Juli 2012.

[10] Ben S Cazzolato and Justin Ghan. Expression for the estimation of time-averaged three-dimensional acoustic energy density spectral density. *The Journal of the Acoustical Society of America*, 2005.

[11] Stefan Weinzierl. *Handbuch der Audiotechnik*. Springer-Verlag Berlin Heidelberg, 2008.

[12] Michael Möser. *Messtechnik der Akustik*. Springer, 1. edition, 2010.

[13] Gerhard Müller and Michael Möser. *Handbook of engineering acoustics*. Springer Berlin Heidelberg, 2013.

[14] SJ Elliott. Errors in acoustic intensity measurements. *Journal of Sound and Vibration*, 78(3):439–443, 1981.

[15] Vinh Trinh. Measurement of sound intensity and sound power. Technical report, Department of Defence - DSTO - Materials research laboratory - Australia, 1993.

[16] PS Watkinson. The practical assessment of errors in sound intensity measurement. *Journal of sound and vibration*, 105(2):255–263, 1986.

[17] Finn Jacobsen. An overview of the sources of error in sound power determination using the intensity technique. *Applied Acoustics*, 50(2):155 – 166, 1997. Sound Intensity Measurement.

[18] J.K. Thompson and D.R. Tree. Finite difference approximation errors in acoustic intensity measurements. *Journal of Sound and Vibration*, 75(2):229 – 238, 1981.

[19] J Pope and JY Chung. Comments on "Finite difference approximation errors in acoustic intensity measurements". *Journal of Sound and Vibration*, 82(3):459–462, 1982.

[20] Hans-Elias de Bree, Peter Leussink, Twan Korthorst, Henri Jansen, Theo SJ Lammerink, and Miko Elwenspoek. The μ-flown: a novel device for measuring acoustic flows. *Sensors and Actuators A: Physical*, 54(1):552–557, 1996.

[21] Finn Jacobsen and Hans-Elias de Bree. A comparison of two different sound intensity measurement principlesa). *The Journal of the Acoustical Society of America*, 118(3):1510–1517, 2005.